# eNeuro

### Research Article: New Research | Cognition and Behavior

# Collateral Projections Innervate the Mammillary Bodies and Retrosplenial Cortex: A New Category of Hippocampal Cells

Lisa Kinnavane<sup>1</sup>, Seralynne D. Vann<sup>1</sup>, Andrew J. D. Nelson<sup>1</sup>, Shane M. O'Mara<sup>2</sup> and John P. Aggleton<sup>1</sup>

<sup>1</sup>School of Psychology, Cardiff University, Cardiff, CF10 3AT, United Kingdom <sup>2</sup>Trinity College Institute of Neuroscience, Trinity College, Dublin, Ireland

DOI: 10.1523/ENEURO.0383-17.2018

Received: 13 November 2017

Revised: 31 January 2018

Accepted: 6 February 2018

Published: 26 February 2018

Author contribution: LK, SDV, AJDN, SMOM and JPA designed Research; LK and AJDN performed Research; LK and JPA wrote the paper.

Funding: http://doi.org/10.13039/100010269Wellcome 103722/Z14/Z WT090954AIA

Conflict of Interest: Authors report no conflict of interest.

The present research was supported by Wellcome: Grant numbers 103722/Z14/Z, WT090954AIA.

**Correspondence to** Dr Lisa Kinnavane, School of Psychology, Tower Building, Park Place, Cardiff University, Cardiff, CF10 3AT, United Kingdom. Phone: +44 2920870197. Email: KinnavaneL@cf.ac.uk

Cite as: eNeuro 2018; 10.1523/ENEURO.0383-17.2018

Alerts: Sign up at eneuro.org/alerts to receive customized email alerts when the fully formatted version of this article is published.

Accepted manuscripts are peer-reviewed but have not been through the copyediting, formatting, or proofreading process.

Copyright © 2018 Kinnavane et al.

This is an open-access article distributed under the terms of the Creative Commons Attribution 4.0 International license, which permits unrestricted use, distribution and reproduction in any medium provided that the original work is properly attributed.

1	Collateral projections innervate the mammillary bodies and
2	retrosplenial cortex: A new category of hippocampal cells
3	
4 5	Abbreviated title: Collateral subiculum projections to limbic sites
6 7 8	Lisa Kinnavane <sup>1*</sup> , Seralynne D. Vann <sup>1</sup> , Andrew J. D. Nelson <sup>1</sup> , Shane M. O'Mara <sup>2</sup> and John P. Aggleton <sup>1</sup>
o 9	<sup>1</sup> School of Psychology, Cardiff University, Cardiff, CF10 3AT, United Kingdom
9	<sup>2</sup> Trinity College Institute of Neuroscience, Trinity College, Dublin 2, Ireland
10	* Corresponding author
12	LK, SDV, AJDN, SMOM and JPA designed Research; LK and AJDN performed
12	Research; LK and JPA wrote the paper
14	Research, Erk and STA whole the puper
15	Key words: anterior thalamic nuclei, cingulate cortex, episodic memory, fornix,
16	subiculum
17	
18	Correspondence to Dr Lisa Kinnavane, School of Psychology, Tower Building, Park
19	Place, Cardiff University, Cardiff, CF10 3AT, United Kingdom.
20	Phone: +44 2920870197
21	Email: <u>KinnavaneL@cf.ac.uk</u>
22	
23	
24	Number of figures: 7
25	Number of extended data figures: 3
26	Abstract word count: 242
27	Significance statement word count: 119
28	Introduction word count: 569
29	Discussion word count: 1767
30	
31	Authors report no conflict of interest
32	
33	Acknowledgements: The present research was supported by Wellcome: Grant
34	numbers 103722/Z14/Z, WT090954AIA.
35	
36	
37	
38	

### 39 Abstract

40 To understand the hippocampus it is necessary to understand the subiculum. Unlike other hippocampal subfields, the subiculum projects to almost all distal hippocampal 41 42 targets, highlighting its critical importance for external networks. The present studies, 43 in male rats and mice, reveal a new category of dorsal subiculum neurons that 44 innervate both the mammillary bodies and the retrosplenial cortex. These bifurcating 45 neurons comprise almost half of the hippocampal cells that project to retrosplenial 46 cortex. The termination of these numerous collateral projections was visualized within 47 the medial mammillary nucleus and the granular retrosplenial cortex (area 29). These 48 collateral projections included subiculum efferents that cross to the contralateral 49 mammillary bodies. Within the granular retrosplenial cortex, the collateral projections form a particularly dense plexus in deep layer II and layer III. This 50 51 retrosplenial termination site co-localized with markers for VGluT2 and neurotensin. 52 While efferents from the hippocampal CA fields standardly collateralize, subiculum 53 projections often have only one target site. Consequently, the many collateral 54 projections involving the retrosplenial cortex and the mammillary bodies present a 55 relatively unusual pattern for the subiculum, which presumably relates to how both 56 targets have complementary roles in spatial processing. Furthermore, along with the 57 anterior thalamic nuclei, the mammillary bodies and retrosplenial cortex are key 58 members of a memory circuit, which is usually described as both starting and 59 finishing in the hippocampus. The present findings reveal how the hippocampus 60 simultaneously engages different parts of this circuit, so forcing an important revision of this network. 61

62

### 63 Significance Statement

64 The hippocampus has both cortical and subcortical connections that are critical for 65 spatial learning in rodents and episodic memory in humans. Chief among these 66 connections are the dense hippocampal inputs to the retrosplenial cortex and 67 mammillary bodies, both of which originate in the subiculum. The present 68 experiments reveal that in rodents approximately half of these retrosplenial 69 projections have collaterals that also innervate the mammillary bodies. Consequently, 70 these two areas share common hippocampal information, despite playing different 71 roles in cognition. These same collateral projections contradict longstanding ideas

about extended, serial hippocampal networks for memory. As these networks are

73 affected from the earliest stages of Alzheimer's disease, when memory disorders first

appear, there is added significance in understanding their precise connectivity.

75

### 76 Introduction

77 Within the hippocampus (dentate gyrus, CA fields, and subiculum), the subiculum has 78 a unique status. Unlike any other subfield, the subiculum projects to almost all 79 external sites innervated by the hippocampus (O'Mara, 2005). In addition, some key 80 hippocampal projections arise almost exclusively from the subiculum. Examples 81 include the dense hippocampal efferents to the mammillary bodies, anterior thalamic 82 nuclei, and retrosplenial cortex (areas 29, 30), which together form an extended 83 limbic network (Rolls, 2015; Bubb et al., 2017). These limbic interconnections have 84 been regarded as vital for emotion (Papez, 1937; MacLean, 1949; Dalgleish, 2004) 85 and, more recently, for spatial memory in rodents and episodic memory in humans 86 (Aggleton et al., 2010; Carlesimo et al., 2011; Ritchey et al., 2015). These same 87 hippocampal connections are also directly implicated in the memory loss that 88 characterizes the earliest stages of Alzheimer's disease (Tan et al., 2013; Aggleton et 89 al., 2016). Consequently, understanding the nature of these hippocampal connections 90 remains a priority.

91

92 A feature of the projections from the various hippocampal CA fields is that they 93 standardly collaterize to innervate multiple sites (Swanson et al., 1981; Donovan & 94 Wyss, 1983). In contrast, projections from the subiculum are typically segregated by 95 their columnar and laminar site of origin (Witter et al., 1990; Ishizuka, 2001; Witter, 96 2006; Christiansen et al., 2016). A consequence is that many subiculum neurons only 97 innervate one target site (Swanson et al., 1981; Donovan & Wyss, 1983; Namura et 98 al., 1994; Naber & Witter, 1998; Wright et al., 2010, 2013). There are, however, 99 reasons to suppose that the hippocampal projections to the retrosplenial cortex and 100 mammillary bodies might prove different, as populations of subiculum neurons that 101 project to these two sites seem to be present in overlapping regions of the subiculum 102 in both rats and monkeys (Van Groen & Wyss, 2003; Kobayashi & Amaral, 2007; 103 Christiansen et al., 2016). For these reasons, the present study began by determining 104 whether the source of these hippocampal projections was indeed from the same region 105 of subiculum, before testing if these two sets of hippocampal efferents remain 106 segregated or whether they provide collateral outputs to both targets. Resolving these 107 issues is valuable as it has been presumed that the retrosplenial cortex and 108 mammillary bodies are concerned with different aspects of hippocampal information 109 processing (Byrne et al., 2007; Dillingham et al., 2015a). One potential basis for this 110 difference would be if they derive information from separate hippocampal outputs. 111 112 The initial experiments, therefore, used multiple fluorescent tracers to determine 113 whether the subiculum projections to the mammillary bodies and retrosplenial cortex 114 arise from the same or different cell populations. One of the axonal tracers used in 115 the present study, unconjugated cholera toxin B subunit (CTB), is transported in both 116 anterograde and retrograde directions. A consequence is that 'collateral-collateral' 117 transport can occur (Chen & Aston-Jones, 1998). This form of transport occurs when 118 a tracer is conveyed retrogradely in one collateral to reach the cell soma, where it is 119 then conveyed anterogradely along other collaterals. This property not only makes it 120 possible to specify the location of the particular collateral terminals under 121 investigation, i.e., in either the mammillary bodies or retrosplenial cortex, but it also 122 becomes possible to look for other collateral projections involving these same 123 terminal sites. In follow-up experiments, surgical disconnections helped to test for 124 whether collateral-collateral tracer transport from the hippocampus had, indeed, 125 occurred. Those findings then led to more precise neurochemical characterizations of 126 these shared limbic pathways. 127

# 128 Methods

129 The principal experiments were performed on 34 adult, male Lister Hooded rats

- 130 weighing 270-320g (Envigo, Bichester, UK). Additional experiments involved two
- adult, male C57BL/6 mice weighing 32 and 35g (bred at Cardiff University). Pairs of
- anatomical tracers were used in combination to allow double fluorescent labelling in
- 133 the same animal. The fluorescent retrograde tracers Fast Blue (FB; Polysciences Inc,
- 134 Warrington, PA, USA), FluoroGold (Santa Cruz Biotechnology, Inc., Dallas, TX,
- 135 USA), Cholera Toxin Subunit B-Alexa Fluor-488 (CTB-488) and Cholera Toxin
- 136 Subunit B-Alexa Fluor-594 (CTB-594; Invitrogen, Waltham, Massachusetts, USA).
- 137 Additionally, unconjugated Cholera Toxin Subunit B (CTB; List Biological

138 Laboratories Inc., Campbell, CA, Product # 103B) was used as it is transported along 139 axons in both anterograde and retrograde directions. This tracer was visualized by 140 immunofluorescence. The tracer pairings were as follows: FB + FG, n = 6; CTB-141 488/CTB-594 + FB, n = 4; CTB in mammillary bodies (MB) + FB in retrosplenial cortex (RSP), n = 5; FB in MB + CTB in RSP, n = 2. Single tracer studies using only 142 143 CTB were also conducted: CTB in RSP, n = 3; CTB in MB only, n = 4. A final, 144 additional set of two adult male Lister Hooded rats received injections of the 145 anterograde tracer, 3 kD biotinylated dextran amine (BDA; Life Technologies Ltd, 146 Paisley, UK) in the dorsal hippocampus to provide additional information about the 147 termination sites of possible collateral connections. All experiments were in 148 accordance with UK Animals (Scientific Procedures) Act, 1986 and associated 149 guidelines, and approved by local ethical committees at Cardiff University. 150 151 Surgical methods - rats 152 All rats were anesthetized throughout surgery with isofluorane (5% for induction, 2% 153 thereafter). Rats were placed in a stereotaxic frame (Kopf, Tujunga, CA, USA), with 154 the mouth-bar set at +5.0mm. For analgesic purposes, Lidocaine was administered 155 topically (0.1ml of 20mg/ml solution; B. Braun, Melsungen, Germany) and 156 meloxicam was given subcutaneously (0.06ml of 5mg/ml solution, Boehringer 157 Ingelheim Ltd, Berkshire, UK). Under aseptic conditions, small openings were made 158 in the skull and dura to allow access for a 0.5µl Hamilton syringe for pressure 159 injections (25ga, Hamilton, Bonaduz Switzerland).

160

161 Single tracer injections (per hemisphere) were made in the mammillary bodies. The

162 coordinates centered on anterior-posterior (AP) -1.9, medial-lateral (ML) +/- 0.5, and

163 dorsal-ventral (DV) -10.4 from bregma, but varied slightly to encompass different

164 subregions. For the retrosplenial cortex, six injections ensured coverage along the full

165 AP plane of this large cortical area. The six coordinates, relative to bregma, with

166 depth relative to top of cortex, were: AP -1.8, ML  $\pm 0.5$ , DV -1.0; AP -2.8, ML  $\pm 0.5$ ,

167 DV -1.0; AP -4.0, ML ±0.5, DV -1.0; AP -5.8, ML ±0.5, DV -2.5; AP-5.8, ML ±0.9,

168 DV -1.4; AP-6.6, ML ±0.9, DV -1.8). Animals received either bilateral or unilateral

169 injections in the same structure.

- 171 Unconjugated-CTB, CTB488 and CTB594 were made up as a 1% solution in sterile 172 0.1M phosphate buffered saline (PBS; pH 7.4), Fast Blue was made up as a 3% 173 solution in sterile PBS (pH 7.4), while FluoroGold was made up as a 4% solution in 174 sterile, distilled water. Following pressure injections of 0.06-0.1 ul into each site, the 175 syringe was left in place for at least five minutes to help reduce any back flow of the 176 tracer. For the retrosplenial cortex there was no concern about tracers travelling back 177 up the syringe tract, however, some evidence of the tracers could be detected from the 178 syringe tracks immediately above the mammillary body injections.
- 179

180 For the anterograde tracer studies, BDA was made up as a 10% solution in sterile,

181 distilled water (pH 7.4) and injections were made at three sites along the anterior-

182 posterior axis of the dorsal subiculum. The injection coordinates relative to bregma

183 were: AP -4.4, ML  $\pm$  2.9, DV -5.8; AP -5.0, ML  $\pm$  3.8, DV -6.7; AP -5.3, ML  $\pm$  4.9,

184 DV -8.3. Injection volumes were  $0.06 - 0.08 \mu$ L. The pressure injections were made

over 10 minutes with the syringe left in place for at least five minutes to help reduceback flow of the tracer.

187

After completion of the tracer injections, the scalp was sutured and animals received a
5 ml subcutaneous injection of 5% glucose in 0.9% saline (Baxter Healthcare Ltd,
Norfolk, UK). Clindamycin hydrochloride antibiotic powder (Fort Dodge Animal
Health Ltd, Southampton, UK) was applied over the closed, sutured scalp. Animals
recovered in a thermostatically controlled container before returning to individual

210 housing with *ad lib* food and water.

211

## 212 Surgical methods – mice

213 The mice were anesthetized throughout surgery with isofluorane (5% for induction,

214 2% thereafter). Mice were placed in a stereotaxic frame using a flat skull orientation.

215 Lidocaine was administered topically (0.1ml of 2mg/ml solution) and meloxicam was

216 given subcutaneously (0.06ml of 0.5mg/ml solution). Under aseptic conditions, small

 $217 \qquad \text{openings were made in the skull and dura to allow access for a 5 \mu l Hamilton syringe}$ 

218 (33ga) connected to a UMP3 microsyringe pump injector (World Precision

219 Instruments, Hertfordshire, UK) with a flow rate of 0.02µl per minute.

- 221 A single tracer injection (CTB, 0.05µl) was made in the mammillary bodies with 222 coordinates AP -2.1, ML +0.2, DV -5.5 from bregma. For the retrosplenial cortex, 223 two ipsilateral Fast Blue injections (both 0.1µl) ensured spread along the cortex. The 224 coordinates, relative to bregma were: AP -1.5, ML  $\pm 0.2$ , DV -0.8; AP -2.4, ML  $\pm 0.2$ , 225 DV -1.0. Post-surgical care was the same as for rats, except that the mice received a 226 0.5 ml subcutaneous injection of 5% glucose in 0.9% saline. 227 228 Testing the collateral – collateral transport of CTB: Fornix lesions 229 Surgical disconnections were used to test whether CTB injected into the mammillary 230 bodies could first be transported retrogradely in the fornix to the hippocampus 231 (subiculum), but then be transported anterogradely in the same subiculum neuron to 232 the retrosplenial cortex ('collateral-collateral transport'). For this reason, in some rats 233 lesions were made in the fornix, followed by CTB tracer injection into the 234 mammillary bodies. Although it was possible to conduct the complementary 235 experiment, i.e., injecting CTB into retrosplenial cortex after fornix lesions, this 236 procedure was not carried out as there are light, direct projections from retrosplenial 237 cortex to the mammillary bodies (Van Groen & Wyss, 2003). 238 239 Bilateral radiofrequency lesions were targeted at the postcommissural descending 240 fornix (n = 4). This region of the fornix was the preferred target as it is the 241 subdivision of the fornix taken by neurons projecting from the subiculum to the 242 mammillary bodies (Swanson & Cowan, 1977). The lesions were made using a 243 thermocouple radiofrequency electrode (0.3 mm active tip length, 0.25 mm diameter; 244 Diros Technology Inc., Ontario, Canada). The electrode was lowered vertically and 245 the tip temperature was then raised to 70-74°C for 45 seconds using an OWL 246 Universal RF System URF-3AP lesion maker (Diros Technology Inc. Ontario, 247 Canada). The stereotaxic coordinates from bregma were: AP -0.2, LM  $\pm$ 1.2, DV -8.4, 248 with the mouth-bar set at + 5.0 mm. 249 250 **Post-operative processing** 251 Following a postoperative period of seven days, the rats were deeply anesthetized
  - 252 with sodium pentobarbital (Euthatal, Merial, Harlow, UK). They were then perfused
  - 253 intracardially with 0.1M PBS at room temperature followed by 4% paraformaldehyde

254	in 0.1M PBS at $\sim$ 4°C. Brains were removed and post-fixed in the dark for 4 hours in
255	paraformaldehyde and then transferred to 25% sucrose solution in 0.1M PBS for 24
256	hours in the dark before sectioning into $40\mu m$ coronal sections with a freezing
257	microtome (Leica 1400). A 1-in-4 series of sections was mounted directly onto
258	gelatine-subbed slides and then allowed to dry in the dark at room temperature. This
259	series was stained with cresyl violet to help localize the injection sites. For the
260	surgical cases involving Fast Blue, FluoroGold, CTB488 or CTB594, a second 1-in-4
261	series was mounted directly onto gelatine-subbed slides, allowed to dry, dehydrated in
262	increasing concentrations of alcohol, then cover-slipped using DPX (Sigma Aldrich,
263	Gillingham, UK).
264	
265	For the cases involving CTB, the second tissue series was immunohistochemically
266	stained for that tracer. The sections were incubated in a solution of rabbit-anti-cholera
267	toxin primary antibody (1:10,000; Sigma Aldrich, Gillingham, UK, Product # C3062,
268	batch 104M4768V; RRID: AB_258833) and 1% normal goat serum in 0.1M PBS for
269	24 hours at room temperature. Following washing, the sections were incubated with
270	DyLight 594 - Goat-anti-Rabbit (1 in 200; Vector Laboratories, Peterborough, UK,
271	Product # DI-1594; RRID: AB_2336413) for 24 hours at 4°C. Sections were then
272	mounted onto gelatine-subbed slides, allowed to dry, dehydrated in increasing
273	concentrations of alcohol and cover-slipped with DPX.
274	
275	For the cases involving BDA, the second tissue series was incubated in the Vectastain
276	ABC solution (Vector Labs, Peterborough, UK) for 2 hours, then washed in PBST
277	twice for 10min each, followed by a further three washes in 0.1M PBS. Sections were
278	then reacted with diaminobenzidine (DAB; Vector Labs, Peterborough, UK) and
279	intensified with nickel, after which they were mounted, dried, and coverslipped, as
280	described above.
281	
282	Sections were viewed using a Leica DM5000B microscope for both transmitted white
283	light (for sections stained with cresyl violet) and fluorescence microscopy (for
284	sections with a fluorophore). An attached Leica DFC350FX digital camera and LAS
285	AF image acquisition software (Leica) were used to capture high resolution images.
286	
287	

### 288 Experimental design and statistical analysis

Fast Blue in conjunction with FluoroGold was used for initial qualitative analyses of the two pathways. For quantitative analyses, Fast Blue injections were paired with CTB injections into the mammillary bodies or retrosplenial cortex. The combination of Fast Blue and CTB was chosen for quantification as these tracers have distinctive emission wavelengths (420nm and 618nm respectively) and fill neuronal cell bodies in different ways (Köbbert et al., 2000). Cell counts were only taken from those animals in which the respective injections were correctly located.

296

297 Double-labelled subicular neurons were counted using the object-based co-

298 localization methods of 'Just Another Co-localization Plugin', a plugin to the public

299 domain, ImageJ software (Bolte & Cordelières, 2006). This software allowed for the

300 initial identification of subicular neurons that project to each region separately. The

301 plugin then determined the fluorescence intensity centers of the CTB-positive

302 subcellular structures and identified the locations at which they coincide with Fast

303 Blue. The system was tested using images that were taken on the same microscope,

304 under the same conditions as the images to be analyzed. These test images had either

305 two overlapping (different fluorophores targeting the same protein) or non-

306 overlapping distributions of fluorescent staining. The co-localization analysis was

307 carried out in four regions of interest across the proximal-distal axis of the dorsal

308 subiculum (see Christiansen et al., 2016). An average of ten dorsal subiculum sections

309 from -5.16 to -6.60 mm posterior to bregma (Paxinos & Watson, 2005) were analyzed

310 for each case. Cell counts were taken from the dorsal subiculum as this is the source

311 of the hippocampal projections to retrosplenial cortex (Van Groen & Wyss, 2003).

312

### 313 Post-operative processing: Additional immunofluorescent targets

314 These analyses examined the sites of collateral-collateral transport termination.

315 Selected targets followed inspection of the Allen Brain Atlas (http://www.brain-

316 map.org). Accordingly, antibodies for Calbindin D28k (1 in 10,000; Swant, Marly,

317 Switzerland, Product # 300; RRID: AB\_10000347), Calretinin (1 in 5,000; Swant,

318 Marly, Switzerland, Product # 6B3; RRID: AB\_10000320), Cholecystokinin 8 (1 in

319 500; Abcam, Cambridge, UK, Product # ab37274; RRID: AB\_726010), GAD67 (1 in

320 1000; Merck Millipore, Hertfordshire, UK, Product # MAB5406; RRID:

321 AB\_2278725), Parvalbumin (1 in 15,000; Sigma-Aldrich, Gillingham, UK, Product #

322 P3088; RRID: AB 477329), Neurotensin (1 in 100; Product # SAB4200703, Sigma-323 Aldrich Gillingham, UK), VGluT1 (1 in 300; Product # ab193595, Abcam, 324 Cambridge, UK), and VGluT2 (1 in 300; Product # ab7915, Abcam, Cambridge, UK) 325 were included. The secondary antibody, DyLight 488 – Horse-anti-mouse (1 in 200; 326 Vector Laboratories, Peterborough, UK, Product # DI-2488; RRID: AB 2307439) 327 was used for visualization. Processing followed standard protocols (see Dillingham et 328 al., 2015b). All antibodies were tested before use to help confirm regional specificity 329 by reference back to the Allen Brain Atlas. Immunohistochemical analyses were 330 conducted on series of tissue from a subset of the surgical cases described above; CTB in MB + FB in RSP, n = 4; FB in MB + CTB in RSP, n = 1; CTB in MB only, n 331 332 = 4.333 334 For the examples of the higher magnification (40x) images of VGluT2 and NT, 335 Manders' coefficient of colocalization was estimated, again using 'Just Another Co-336 localization Plugin' (Bolte & Cordelières, 2006). The M<sub>1</sub> quantifies the proportion of 337 the green signal coincident with a signal in the red channel over its total intensity. 338 This measure can fall between zero (no overlap) and one (complete colocalization). 339 340 **Anatomical nomenclature** 341 Anatomical names and borders follow Swanson (1992), except for the divisions 342

within the retrosplenial cortex and postsubiculum, which use the terminology of Van 343 Groen and Wyss (2003). The latter authors divide retrosplenial cortex into a dorsal, 344 dysgranular subregion (Rdg, area 30) and two ventral, granular subregions (Rga, Rgb, 345 area 29). [Note, other authors further subdivide area 29, e.g., Jones and Witter 346 (2007).] Here, the rat subiculum is divided into two layers, i.e., a superficial 347 molecular layer and a deeper, thick layer of pyramidal cells (Kloosterman et al., 348 2003). The term 'intermediate subiculum' refers to that subiculum region at the 349 caudal extent of the hippocampal flexure where the dorsal subiculum and ventral 350 subiculum converge (Bast et al., 2006). In accordance with Witter and Wouterlood 351 (2002), the subiculum is included within the hippocampus, while the presubiculum, 352 parasubiculum (and postsubiculum) form parts of the parahippocampal region. 353

- 354
- 355

### 356 **Results**

357 In an initial series (n = 3), injections of Fast Blue and FluoroGold helped to confirm 358 the presence of overlapping populations of dorsal subiculum neurons that project to 359 the two target regions (Figure 1D). Within these overlapping populations of 360 pyramidal cells (blue to retrosplenial cortex, yellow to mammillary bodies), some 361 cream colored cells were observed (Figure 1D). These additional neurons are 362 presumed to send axons to both the mammillary bodies and retrosplenial cortex. A 363 similar pattern of results was obtained with the reverse tracer-target configuration (n =364 3). This pattern was further corroborated using Cholera Toxin Subunit B conjugated 365 to Alexa Fluors (CTB488 and CTB594), in combination with either Fast Blue or 366 FluoroGold (n = 4). 367 368 To quantify this population of collateralizing projections more precisely, Fast Blue 369 and CTB were separately injected into the two target sites (Figure 1B,C). Of the 370 acceptable injections, five involved CTB in the mammillary bodies and Fast Blue in 371 retrosplenial cortex, while two rats received the reverse placement of tracers. Double-

labelling was observed in pyramidal cells in the middle of layer II of the septal andintermediate (dorsal) subiculum (Figure 1A). The number of labelled neurons was

374 estimated in four regions of interest along the proximal-distal axis of the subiculum

375 (R1-4; Figure 2). Double-labelled neurons were most prevalent in the mid proximal-

distal plane (R2 and R3) of the dorsal hippocampus (Figure 1A, 2). The cell counts

from these seven cases indicated that an overall mean of 46% (range 41.8% to 64.3%)

378 of the subiculum pyramidal neurons that project to the retrosplenial cortex also

379 collateralize to innervate the mammillary bodies (Figure 2; Extended Data Figure 2-

380 1). (This percentage is an underestimate as complete mammillary body tracer uptake

381 would be needed for a full count.) No apparent morphological characteristics could

382 be discerned to distinguish single from double-labelled cells.

383

384 After being transported retrogradely to the subiculum, CTB can travel anterogradely

385 in the same neuron (Chen & Aston-Jones, 1998), labelling its collateral terminal fields

386 (Figure 3A,B). Consequently, four more rats received a CTB injection in the

387 mammillary bodies, while three received CTB in the retrosplenial cortex. The

388 mammillary body CTB injections not only retrogradely labelled numerous cells in the

389 subiculum of both hemispheres, but also produced a dense band of bilateral terminal 390 label throughout deep layer II and layer III of granular retrosplenial cortex (Figure 391 3A). This terminal label in areas 29a and 29b stopped abruptly at the border with 392 dysgranular retrosplenial cortex (area 30). This pattern of terminal labelling matches 393 that produced when an anterograde tracer such as BDA is injected into the dorsal 394 subiculum (Figure 3E-G), thus, is consistent with the direct projections from 395 subiculum to retrosplenial cortex. Meanwhile, CTB injections in retrosplenial cortex 396 led to ipsilateral, dorsal subiculum label, accompanied by (bilateral) terminal label in 397 the medial mammillary nucleus, most evident in dorsal pars lateralis (Figure 3B). 398

399 In those cases with CTB injections in the mammillary bodies it was possible to look 400 for anterograde label in other sites that do not receive direct mammillary inputs, as 401 such label might reflect additional collateral connections. (The same procedure was 402 not applied to those cases with CTB injections in retrosplenial cortex as, unlike the 403 mammillary bodies, this cortical region innervates many different sites, so making 404 interpretation more difficult.) As expected, dense anterograde label was observed in 405 the anterior thalamic nuclei due to the very large projection via the mammillothalamic 406 tract (Figure 3C). Other sites containing terminal label included the prelimbic cortex, 407 infralimbic cortex, the septum (medial and lateral), and the medial and lateral regions 408 of entorhinal cortex (Figure 3D). This entorhinal label was concentrated in the deep 409 layers, predominantly in layer V.

410

### 411 Testing the collateral-collateral transport of CTB: Fornix lesions

412 In those cases with the most complete section of the postcommissural descending 413 fornix (compare Figure 4A with 4B), the quantity of retrograde subiculum label was 414 markedly attenuated after CTB injections in the mammillary bodies (Figure 4C,D). In 415 these cases (n = 2), the anterograde label in area 29 was no longer visible (Figure 4E). 416 This result, the elimination of terminal label in retrosplenial cortex, indicated that the 417 anterograde label had originated via the subiculum inputs to the mammillary bodies. 418 To confirm that this absence of tracer signal in the subiculum and retrosplenial cortex 419 was not due to the tracer failing to be taken up by the mammillary bodies following 420 fornix lesions, Gudden's ventral tegmental nucleus was examined as this nucleus 421 projects to the mammillary bodies, but not via the fornix (Allen & Hopkins, 1989).

422 Comparable numbers of neurons labelled with CTB were observed in Gudden's

- 423 nucleus, whether the fornix had been cut or spared (Figure 4F,G), confirming tracer
- 424 uptake in both conditions.
- 425
- 426

## 427 Cross-hemispheric collateral projections

428 The pattern of double and single labelling in the subiculum following tracer injections 429 into one hemisphere indicated that the projections to the retrosplenial cortex remained 430 ipsilateral to the subiculum while the collaterals to the mammillary bodies could arise 431 from either the ipsilateral or contralateral subiculum.

432

### 433 Cross-species comparisons

434 To determine whether these bifurcating subicular neurons are present in other rodents, 435 the same anatomical methods were applied to adult mice (C57BL/6 strain). The tracer 436 CTB was injected into the mammillary bodies (Figure 5A) and Fast Blue injected into 437 the retrosplenial cortex (Figure 5B) generating a population of double-labelled 438 neurons in the dorsal subiculum (Figure 5C). Quantification of those subiculum 439 neurons that project to retrosplenial cortex and also project to the mammillary bodies 440 yielded remarkably similar results to those found in the rat (Extended Data Figure 5-441 1). The co-localization analysis indicated that an overall mean of 41% of those 442 subiculum neurons that project to retrosplenial cortex also collateralize to innervate

the mammillary bodies (range across cases 39.8% - 46.5%). Furthermore, CTB tracer

444 injections in the mammillary bodies again resulted in dense terminal label, restricted

to area 29 (Figure 5D). This label was concentrated in deep layer II and layer III

446 (Figure 5D), consistent with collateral-collateral transport via the subiculum and the

447 results seen in the rat.

448

## 449 Neurochemistry of subiculum efferents

450 The ability to visualize the collateral projections within retrosplenial cortex made it

451 possible to determine if these subiculum efferents co-localize with specific

452 neurochemicals. Using tissue from rats with CTB injections in the mammillary

453 bodies, immunofluorescence revealed how the area 29 terminations specifically co-

454 localized with signals for VGluT2 and neurotensin (Figure 6A,B). This co-

455 localization was very precise as both VGluT2 and neurotensin matched the CTB

456 distribution in deep layer II and III, but appeared absent from the rest of area 29. The

457 co-localization in Figure 6 was estimated using Manders' Coefficient; for VGluT2 458 signal overlap with the CTB signal was  $M_1 = 0.72$ , while for neurotensin the overlap 459 with CTB was M1 = 0.96. Signals for neurotensin and VGluT2 were also present in 460 dorsal pars lateralis of the medial mammillary bodies, i.e., those regions receiving 461 collateral innervations. The CTB-positive area 29 terminations did not co-localize 462 with VGluT1, GAD67, calretinin, parvalbumin (PV), calbindin, or cholecystokinin 463 (Extended Data Figure 6-1).

464

465 As has been described previously (Varoqui et al., 2002), we found a paucity of 466 VGluT1 label in deep layer II and layer III. GAD67 is a GABA-synthesizing enzyme 467 and so was employed as a crude marker for GABAergic neurons to be followed up by 468 other interneuron markers. GAD67 and CTB-positive terminals showed an almost 469 complementary pattern of staining with GAD67 present in superficial layer II and the 470 deeper cortical layers but not deep layer II and III (Extended Data Figure 6-1). The 471 pattern of PV labelling was, unsurprisingly, very similar to that of GAD67. Although 472 non-overlapping, there was a close association with CTB terminals in area 29 and PV-473 positive staining as PV cell bodies were found to sit among the CTB-positive 474 terminals in deep layer II and adjacent to PV-positive terminals in superficial layer II 475 (Extended Data Figure 6-1); this pattern of PV staining matches previous descriptions 476 (Salaj et al., 2015). Also consistent with previous reports (Salaj et al., 2015), 477 calretinin had low but detectable levels of staining of both cells bodies and neuropil in 478 retrosplenial cortex but there was a conspicuous absence of label in layers II and III, 479 and so no overlap with CTB. The final interneuron markers to be tested, calbindin and 480 cholecystokinin, had very low levels of expression in retrosplenial cortex. Taken 481 together, these results show that these CTB-labelled projections are excitatory rather 482 than inhibitory. 483

### 484 **Discussion**

The present study revealed collateral subiculum projections that simultaneously link the hippocampus with two sites, the mammillary bodies and the retrosplenial cortex (Figures 1, 2). These shared projections arise from the dorsal subiculum, comprising almost half of the hippocampal projections to retrosplenial cortex in both rats and mice. For some of these collateral projections, the input from the subiculum to the

490	mammillary bodies crosses to the opposite hemisphere (Figure 7A). Meanwhile, the
491	retrograde then anterograde movement of CTB, the latter via collateral-collateral
492	transport, showed how the termination sites of these collateral projections are
493	restricted to the medial mammillary nucleus and retrosplenial area 29 (layers deep II
494	and III) (Figure 3). Consequently, these two sites receive shared hippocampal
495	information, despite the different contributions they make to learning and memory
496	(Byrne et al., 2007; Vann et al., 2009; Dillingham et al., 2015a, Roy et al., 2017).
497	This finding of a new category of subiculum neurons may relate to recent
498	electrophysiological descriptions of multiple subpopulations of spatial cells within
499	this same hippocampal region (Brotons-Mas, et al., 2017).
500	
501	At the outset, it is important to confirm whether the CTB injections did, indeed, result
502	in collateral-collateral transport, as such label best specifies the terminal sites of
503	hippocampal collaterals within the retrosplenial cortex and mammillary bodies. The
504	clearest evidence relates to the anterograde label observed in retrosplenial cortex
505	following CTB injections into the mammillary bodies. First, there are no direct
506	projections from the mammillary bodies to retrosplenial cortex (Van Groen & Wyss,
507	2003) and although transneuronal tracing has been observed using a biotin conjugate
508	of CTB (Lai et al., 2015), unconjugated CTB is not thought to be trans-synaptically
509	transported under the conditions used in the present study (Bilsland & Schiavo, 2009).
510	While one potential trans-synaptic route would have been via the anterior thalamic
511	nuclei, this would have principally produced anterograde label in layers I and V of
512	retrosplenial cortex (Van Groen & Wyss, 2003). Instead, the observed label was
513	restricted to layers II and III. Second, the distribution of the retrosplenial terminal
514	label precisely matched that of the direct projections from the subiculum to
515	retrosplenial cortex (Figure 3F, see also Van Groen & Wyss, 2003). Perhaps, most
516	compelling, was the finding that surgical disconnection of the hippocampal
517	projections to the mammillary bodies blocked the presence of this terminal label in
518	retrosplenial cortex.
519	
520	Evidence of transport of CTB from the retrosplenial cortex to the subiculum, and then
521	to the medial mammillary bodies, was also observed, but this potential collateral-
522	collateral label is more difficult to interpret. The difficulty arises because there is a

523 very light, direct projection from granular retrosplenial cortex to the mammillary

524 bodies (Van Groen & Wyss, 1990, 2003; see also retrograde labelled neurons in 525 Figure 3A). The apparent co-localization of the CTB label in the medial mammillary 526 nucleus with neurotensin is consistent with this being collateral-collateral transport, 527 but not proof. Likewise, the finding that the CTB label was concentrated in the dorsal 528 medial mammillary nucleus is more consistent with a projection from the septal 529 (dorsal) subiculum (Shibata, 1989; Kishi et al., 2000), especially as the sparse, direct 530 retrosplenial inputs from Rga are scattered across the mammillary bodies (Van Groen 531 & Wyss, 1990).

532

533 The collateral-collateral transport of CTB made it possible to look for other 534 projections to the mammillary bodies that might collateralize, e.g., from the 535 subiculum. The mammillary bodies lend themselves to this analysis as they only have 536 a restricted set of efferent targets. Aside from the anterior thalamic nuclei, which 537 receive especially dense, direct projections from the mammillary bodies, other sites 538 containing terminal label included the medial and lateral regions of entorhinal cortex, 539 as well as the infralimbic and prelimbic cortices. Of these sites, the entorhinal label is 540 the most likely to reflect collateral-collateral connections via the subiculum as the 541 other sites receive direct mammillary body inputs (Hoover & Vertes, 2007). 542 Furthermore, subiculum neurons that innervate both the mammillary bodies and 543 entorhinal cortex have already been described (Donovan & Wyss, 1983; Roy et al., 544 2017). As the subiculum inputs to entorhinal cortex terminate in the deep layers 545 (Sorensen & Shipley, 1979), this distribution is consistent with the present entorhinal 546 terminal label reflecting collateral projections. It was, therefore, striking that the 547 density of this terminal label in entorhinal cortex appeared far less than that seen in 548 retrosplenial cortex (Figure 3A,D), even when accounting for the more diffuse 549 termination zone. Meanwhile, the value of appreciating hippocampal collateral 550 projections has been highlighted by recent studies with mice. Roy et al. (2017) 551 demonstrated the importance of subiculum neurons that collateralize to both the 552 entorhinal cortex and mammillary bodies for fear memory retrieval (subiculum to 553 entorhinal cortex) and for coincident fear states associated with fear memory retrieval 554 (subiculum to mammillary bodies). They suggest that in their contextual fear 555 conditioning paradigm the dorsal subiculum to mammillary body projections regulate 556 memory-retrieval-induced stress hormone responses, although it should be pointed 557 out that the mammillary bodies have been implicated in many forms of spatial

memory that do not involve an overtly stressful component (Vann & Aggleton, 2004;
Vann & Nelson, 2015).

560

It should be added that the postsubiculum and regions of the medial prefrontal cortex also project to both mammillary bodies and retrosplenial cortex. Examination of these areas in our paired tracer studies revealed single labelled neurons but not doublelabelled neurons. Thus, neurons in these regions are unlikely to contain neurons that collateralize to mammillary bodies and retrosplenial cortex.

566

567 The collateral-collateral transport of CTB also demonstrated the striking overlap 568 between the collateral projections to area 29 and the presence of neurotensin and 569 VGluT2, but not VGluT1. With known neurotensin projections from the subiculum 570 to both the retrosplenial cortex and the mammillary bodies (Roberts et al., 1984; 571 Kiyama et al., 1986), it now appears very likely that many of these same connections 572 collaterize. Meanwhile, VGluT1 and VGluT2, which reflect different subclasses of 573 glutamate terminal (Fremeau et al., 2004), occupy complementary areas within 574 granular retrosplenial cortex (Varoqui et al., 2002). Their respective laminar 575 locations within retrosplenial cortex are notable as they differ appreciably from that 576 found across other cortical areas (Varoqui et al., 2002). Our tissue also indicates that 577 the collateral subiculum projections to the mammillary bodies are again VGluT2 and 578 neurotensin-positive (see also Ziegler et al., 2002). Neurotensin can act as a 579 neuromodulator to several neurotransmitter systems, including the glutamatergic 580 system. A microdialysis study in freely moving rats demonstrated that neurotensin 581 enhances cortical glutamate release, particularly by modulating the functional activity 582 of cortical NMDA receptors (Ferraro et al., 2011). Thus, perhaps amplifying the 583 excitatory signals from the hippocampus to these regions. While the analysis of these 584 terminals permitted precise visualization of these subiculum-limbic efferents, it was 585 not, however, possible to determine if the collateral projections have properties that 586 differ from those connections that only reach one target. 587

588 The present findings challenge notions about subiculum organization. Previous

589 studies have shown that many subiculum connections are segregated by their

590 columnar and laminar origin (Witter et al., 1990; Ishizuka, 2001; Witter, 2006; Wright

591 et al., 2010, 2013; Christiansen et al., 2016), consequently subiculum neurons often 592 innervate only one target. This property provides a marked contrast with the adjacent 593 hippocampal CA fields (Swanson et al., 1981; Naber & Witter, 1998). The present 594 findings now, however, show that the hippocampal (subiculum) inputs to the 595 mammillary bodies may provide a special case as some of these inputs have 596 collaterals to the retrosplenial cortices (present study) while, as others have already 597 noted, there are also subiculum projections to the mammillary bodies with collaterals 598 to the entorhinal cortex (Donovan & Wyss, 1983). In this way, subiculum neurons 599 that collaterize link the hippocampus simultaneously with other sites that make 600 different contributions to cognition (Vann et al., 2009; Todd & Bucci, 2015; Roy et 601 al., 2017).

602

603 With respect to spatial processing, the mammillary bodies are closely linked with 604 learning allocentric-based locations and providing head direction information, while 605 the retrosplenial cortex is closely linked to landmark usage and changing reference 606 frames (Vann & Aggleton, 2004; Byrne et al., 2007; Auger et al., 2012; Dillingham et 607 al., 2015a; Vann & Nelson, 2015). Retrosplenial cortex also contains cells coding for 608 spatial context (Mao et al., 2017), as well as head direction cells linked to landmarks 609 (Jacob et al., 2017). The mechanisms behind these complementary spatial functions 610 become more tractable in light of the discovery of shared hippocampal projections to 611 both sites. These same complementary features also highlight the key position of the 612 anterior thalamic nuclei, which receive dense inputs from both the mammillary bodies 613 and retrosplenial cortex, as well as the hippocampus. Consistent with this strategic 614 location and the partial duplication of hippocampal inputs to the mammillary bodies 615 and retrosplenial cortex, lesion studies in rats have shown that the anterior thalamic 616 nuclei are more critical for hippocampal-sensitive spatial tasks than either the 617 mammillary bodies or retrosplenial cortex (Aggleton et al., 1991, 1995; Neave et al., 618 1994). In addition, these thalamic nuclei show additional electrophysiological 619 properties relating to spatial information (Tsanov et al., 2011; Jankowski et al., 2015) 620 than either the mammillary bodies or retrosplenial cortex. These findings are 621 consistent with the convergent involvement of the anterior thalamic nuclei in multiple 622 aspects of spatial learning, which is partly fed by the collateral subiculum projections 623 to the mammillary bodies and retrosplenial cortex.

624

625	The mammillary bodies, anterior thalamic nuclei, and retrosplenial cortex are key
626	steps along a hippocampal return circuit ('Papez circuit') historically presumed to be
627	vital for emotion (Dalgleish, 2004; see Figure 7B). These same sequential
628	connections also provide the core of an extended hippocampal-limbic circuit, critical
629	for episodic memory (Aggleton & Brown, 2006; Carlesimo et al., 2011; Rolls, 2015).
630	The finding of a bifurcating pathway that allows the hippocampus to influence the
631	diencephalon (mammillary bodies) and cingulate gyrus (retrosplenial cortex) either
632	individually or in parallel (Figure 7B), presents a different perspective. Indeed, in
633	conjunction with other neuroanatomical studies (Jones & Witter, 2007; Kobayashi &
634	Amaral, 2007), there is need to markedly revise this hippocampal-limbic circuit.
635	Three parallel hippocampal-anterior thalamic routes emerge in this new account
636	(Figure 7B). First, a 'ventral' subcortical route, via the fornix to the mammillary
637	bodies and anterior thalamic nuclei, i.e., the original Papez circuit. Second, a 'dorsal'
638	cortical route, containing multiple two-way interconnections between the subiculum,
639	retrosplenial cortex, and anterior thalamus (Bubb et al., 2017). Third, the new
640	collateral pathway that unites both the 'ventral' and 'dorsal' routes. These findings
641	create novel hippocampal networks for information processing in the thalamus,
642	cingulate cortices, and beyond. These anatomical insights are timely as growing
643	evidence links episodic memory loss in Mild Cognitive Impairment and early
644	Alzheimer's disease with the breakdown of this same extended hippocampal network
645	(Tan et al., 2013; Aggleton et al., 2016).
646	
647	
648	References
649	Aggleton JP, Brown MW (2006) Interleaving brain systems for episodic and
650	recognition memory. Trends Cogn Sci 10:455-463.
651	Aggleton JP, Keith AB, Sahgal A (1991) Both fornix and anterior thalamic, but not
652	mammillary, lesions disrupt delayed nonmatching-to-position memory in rats.
653	Behav. Brain Res 44:151-161.
654	Aggleton JP, Neave NJ, Nagle S, Hunt PR (1995) A comparison of the effects of
655	anterior thalamic, mamillary body and fornix lesions on reinforced spatial
656	alternation. Behav Brain Res 68:91-101.

657	Aggleton JP, O'Mara SM, Vann SD, Wright NF, Tsanov M, Erichsen JT (2010)
658	Hippocampal-anterior thalamic pathways for memory: uncovering a network of
659	direct and indirect actions. Eur J Neurosci 31(12):2292-2307.
660	Aggleton JP, Pralus A, Nelson AJD Hornberger M (2016) Thalamic pathology and
661	memory loss in early Alzheimer's disease: moving the focus from the medial
662	temporal lobe to Papez circuit. Brain 139:1877-1890.
663	Allen GV, Hopkins DA (1989) Mamillary body in the rat: Topography and
664	synaptology of projections from the subicular complex, prefrontal cortex, and
665	midbrain tegmentum. J Comp Neurol 286:311-336.
666	Auger SD, Mullally SL, Maguire EA (2012) Retrosplenial cortex codes for permanent
667	landmarks. PloS one 7(8):e43620.
668	Bast T, Wilson IA, Witter MP Morris RGM (2009) From rapid place learning to
669	behavioral performance: a key role for the intermediate hippocampus. PLoS Biol
670	7:e1000089.
671	Bilsland LG, Schiavo G (2009) Axonal Transport Tracers. In: Encyclopedia of
672	Neuroscience (Squire LR, ed), pp1209-1216. Academic Press, Oxford.
673	Bolte S, Cordelières FP (2006) A guided tour into subcellular colocalization analysis
674	in light microscopy. J Microsc 224:213-232.
675	Brotons-Mas JR, Schaffelhofer S, Guger C, O'Mara SM, Sanchez-Vives MV (2017)
676	Heterogeneous spatial representation by different subpopulations of neurons in
677	the subiculum. Neuroscience 343:174-189.
678	Bubb EJ, Kinnavane L, Aggleton JP (2017) Hippocampal-diencephalic-cingulate
679	networks for memory and emotion: An anatomical guide. Brain Neurosci
680	Advances 1:2398212817723443.
681	Byrne P, Becker S, Burgess N (2007) Remembering the past and imagining the
682	future: a neural model of spatial memory and imagery. Psychol Rev 114(2):340-
683	375.
684	Carlesimo GA, Lombardi MG, Caltagirone C (2011) Vascular thalamic amnesia: a
685	reappraisal. Neuropsychologia 49:777-789.
686	Chen S, Aston-Jones G (1998) Axonal collateral-collateral transport of tract tracers in
687	brain neurons: false anterograde labelling and useful tool. Neuroscience
688	82:1151-1163.
689	Christiansen K, Dillingham CM, Wright NF, Saunders RS, Vann SD, Aggleton JP
690	(2016) Complementary subicular pathways to the anterior thalamic nuclei and

691	mammillary bodies in the rat and macaque monkey brain. Eur J Neurosci
692	43:1044-1061.
693	Dalgleish T (2004). The emotional brain. Nat Rev Neurosci 5:583-589.
694	Dillingham CM, Frizzati A, Nelson AJ, Vann SD (2015a) How do mammillary body
695	inputs contribute to anterior thalamic function? Neurosci Biobehav Rev 54:108-119.
696	Dillingham CM, Holmes JD, Wright NF, Erichsen JT, Aggleton JP, Vann SD (2015b)
697	Calcium-binding protein immunoreactivity in Gudden's tegmental nuclei and the
698	hippocampal formation: differential co-localization in neurons projecting to the
699	mammillary bodies. Front Neuroanat 9:103.
700	Donovan MK, Wyss JM (1983) Evidence for some collateralization between cortical
701	and diencephalic efferent axons of the rat subicular cortex. Brain Res 259:181-
702	192.
703	Ferraro L, Beggiato S, Tomasini MC, Fuxe K, Tanganelli S, Antonelli T (2011)
704	Neurotensin regulates cortical glutamate transmission by modulating N-methyl-
705	D-aspartate receptor functional activity: an in vivo microdialysis study. J
706	Neurosci Res 89(10):1618-1626.
707	Fremeau RT, Voglmaier S, Seal RP, Edwards RH (2004) VGLUTs define subsets of
708	excitatory neurons and suggest novel roles for glutamate. Trends Neurosci
709	27(2):98-103.
710	Hoover WB, Vertes RP (2007) Anatomical analysis of afferent projections to the
711	medial prefrontal cortex in the rat. Brain Struct Function 212(2):149-179.
712	Jacob PY, Casali G, Spieser L, Page H, Overington D, Jeffery K (2017) An
713	independent, landmark-dominated head direction signal in dysgranular
714	retrosplenial cortex. Nat Neurosci 20(2):173-175.
715	Jankowski MM, Passecker J, Nurul Islam MD, Vann SD, Erichsen J, Aggleton JP,
716	O'Mara SM (2015) Evidence for spatially-responsive neurons in the rostral
717	thalamus. Front Behav Neurosci 9:256. doi:10.3389/fnbeh.2015.00256.
718	Jones BF, Witter MP (2007) Cingulate cortex projections to the parahippocampal
719	region and hippocampal formation in the rat. Hippocampus 17:957-976.
720	Ishizuka N (2001) Laminar organization of the pyramidal cell layer of the subiculum
721	in the rat. J Comp Neurol 435(1):89-110.
722	Kishi T, Tsumori T, Ono K, Yokota S, Ishino H, Yasui Y (2000) Topographical
723	organization of projections from the subiculum to the hypothalamus in the rat. J
724	Comp Neurol 419(2):205-222.

725	Kiyama H, Shiosaka S, Sakamoto N, Michel JP, Pearson J, Tohyama M (1986) A
726	neurotensin-immunoreactive pathway from the subiculum to the mammillary
727	body in the rat. Brain Res 375(2):357-359.
728	Kloosterman F, Witter MP, Van Haeften T (2003) Topographical and laminar
729	organization of subicular projections to the parahippocampal region of the rat. J
730	Comp Neurol 455:156-171.
731	Kobayashi Y, Amaral DG (2007) Macaque monkey retrosplenial cortex: III. Cortical
732	efferents. J Comp Neurol 502:810-833.
733	Köbbert C, Apps R, Bechmann I, Lanciego JL, Mey J, Thanos S (2000) Current
734	concepts in neuroanatomical tracing. Progress Neurobiol 62(4):327-351.
735	Lai BQ, Qiu XC, Zhang K, Zhang RY, Jin H, Li G, Shen HY, Wu JL, Ling EA, Zeng
736	YS (2015) Cholera toxin B subunit shows transneuronal tracing after injection in
737	an injured sciatic nerve. PLoS One 10(12):e0144030.
738	MacLean PD (1949) Psychosomatic disease and the 'visceral brain'. Psychosom Med
739	11:338-353.
740	Mao D, Kandler S, McNaughton BL, Bonin V (2017) Sparse orthogonal population
741	representation of spatial context in the retrosplenial cortex. Nature Comm 8:243.
742	Naber PA, Witter MP (1998) Subicular efferents are organized mostly as parallel
743	projections: A double-labeling, retrograde-tracing study in the rat. J Comp Neurol
744	393(3):284-297.
745	Neave N, Lloyd S, Sahgal A, Aggleton JP (1994) Lack of effects of lesions in the
746	anterior cingulate cortex and retrosplenial cortex on tests of spatial memory in the
747	rat. Behav Brain Res 65:89-101.
748	Namura S, Takada M, Kikuchi H, Mizuno N (1994) Topographical organization of
749	subicular neurons projecting to subcortical regions. Brain Res Bull 35(3):221-
750	231.
751	O'Mara S (2005) The subiculum: what it does, what it might do, and what
752	neuroanatomy has yet to tell us. J Anat 207:271-282.
753	Papez JW (1937) A proposed mechanism of emotion. Arch Neurol Psychiat
754	38(4):725-743.
755	Paxinos G, Watson C (2005) The rat brain in stereotaxic coordinates: San Diego, CA:
756	Elsevier Academic Press.
757	Ritchey M, Libby LA, Ranganath C (2015) Cortico-hippocampal systems involved in
758	memory and cognition: the PMAT framework. Prog Brain Res 219:45-64.

759	Roberts GW, Woodhams PL, Polak JM, Crow TJ (1984) Distribution of
760	neuropeptides in the limbic system of the rat: the hippocampus. Neuroscience
761	11(1):35-77.
762	Rolls ET (2015) Limbic systems for emotion and for memory, but no single limbic
763	system. Cortex 62:119-157.
764	Roy DS, Kitamura T, Okuyama T, Ogawa SK, Sun C, Obata Y, Tonegawa S (2017)
765	Distinct neural circuits for the formation and retrieval of episodic memories. Cell
766	170(5):1000-1012.
767	Salaj M, Druga R, Cerman J, Kubova H, Barinka F (2015) Calretinin and parvalbumin
768	immunoreactive interneurons in the retrosplenial cortex of the rat brain: Qualitative
769	and quantitative analyses. Brain Res 1627:201-215.
770	Shibata H (1989) Descending projections to the mammillary nuclei in the rat, as studied
771	by retrograde and anterograde transport of wheat germ agglutinin-horseradish
772	peroxidase. J Comp Neurol 285(4):436-452.
773	Shibata H (1993) Efferent projections from the anterior thalamic nuclei to the cingulate
774	cortex in the rat. J Comp Neurol 330(4):533–542.
775	Sørensen KE, Shipley MT (1979) Projections from the subiculum to the deep layers of the
776	ipsilateral presubicular and entorhinal cortices in the guinea pig. J Comp Neurol
777	188(2):313-333.
778	Swanson LW (1992) Brain maps: Structure of the rat brain. Amsterdam: Elsevier.
779	Swanson LW, Cowan WM (1977) An autoradiographic study of the organization of
780	the efferent connections of the hippocampal formation in the rat. J Comp Neurol
781	172(1):49–84.
782	Swanson LW, Sawchenko PE, Cowan WM (1981) Evidence for collateral projections
783	by neurons in Ammon's horn, the dentate gyrus, and the subiculum: a multiple
784	retrograde labeling study in the rat. J Neurosci 1(5):548-559.
785	Tan RH, Wong S, Hodges JR, Halliday GM, Hornberger M (2013) Retrosplenial
786	cortex (BA 29) volumes in behavioral variant frontotemporal dementia and
787	Alzheimer's disease. Dement Geriatr Cogn 35(3-4):177-182.
788	Todd TP, Bucci DJ (2015) Retrosplenial cortex and long-term memory: molecules to
789	behavior. Neural Plasticity 2015:414173. doi: 10.1155/2015/414173.
790	Tsanov M, Vann SD, Erichsen JT, Wright N, Aggleton JP, O'Mara SM (2011)
791	Differential regulation of synaptic plasticity of the hippocampal and the
792	hypothalamic inputs to the anterior thalamus. Hippocampus 21(1):1-8.

793	Van Groen T, Wyss JM (1990) Connections of the retrosplenial granular a cortex in
794	the rat. J Comp Neurol 300:593-606.
795	Van Groen T, Wyss JM (2003) Connections of the retrosplenial granular b cortex in
796	the rat. J Comp Neurol 463:249-263.
797	Vann SD, Aggleton JP (2004). The mammillary bodies: two memory systems in one?
798	Nat Rev Neurosci 5(1):35-44.
799	Vann SD, Aggleton JP, Maguire EA (2009) What does the retrosplenial cortex do?
800	Nat Rev Neurosci 10(11):792-802.
801	Vann, SD, Nelson AJ (2015). The mammillary bodies and memory: more than a
802	hippocampal relay. Progr Brain Res, 219:163-185.
803	Varoqui H, Schäfer MKH, Zhu H, Weihe E, Erickson JD (2002) Identification of the
804	differentiation-associated Na+/PI transporter as a novel vesicular glutamate
805	transporter expressed in a distinct set of glutamatergic synapses. J Neurosci
806	22(1):142-155.
807	Witter MP (2006) Connections of the subiculum of the rat: topography in relation to
808	columnar and laminar organization. Behav Brain Res 174:251-264.
809	Witter MP, Ostendorf RH, Groenewegen HJ (1990) Heterogeneity in the dorsal
810	subiculum of the rat. Distinct neuronal zones project to different cortical and
811	subcortical targets. Eur J Neurosci 2(8):718-725.
812	Witter MP, Wouterlood FG (2002) The parahippocampal region: Organization and
813	role in cognitive function. Oxford: Oxford University Press.
814	Wright NF, Erichsen JT, Vann SD, O'Mara SM, Aggleton JP (2010). Parallel but
815	separate inputs from limbic cortices to the mammillary bodies and anterior
816	thalamic nuclei in the rat. J Comp Neurol 518(12):2334-2354.
817	Wright NF, Vann SD, Erichsen JT, O'Mara S, Aggleton JP (2013) Segregation of
818	parallel inputs to the anteromedial and anteroventral thalamic nuclei of the rat. J
819	Comp Neurol 521:2966-2986.
820	Ziegler DR, Cullinan WE, Herman JP (2002) Distribution of vesicular glutamate
821	transporter mRNA in rat hypothalamus. J Comp Neurol 448(3):217-229.
822	
823	
824	
825	
000	

### 827 Figure Legends

828 Figure 1. Subicular neurons collateralize to innervate the retrosplenial cortex and 829 mammillary bodies. A. Coronal photomicrographs of dorsal subiculum in a rat 830 following Fast Blue (FB) injections in retrosplenial cortex (RSP) and Cholera Toxin 831 B (CTB) in the mammillary bodies (MB) with pink double-labelled cells in the 832 overlay panel indicating neurons that collateralize to both regions. Proximal-distal 833 regions (R1-4) were divisions used for subsequent quantification. B. Coronal section 834 showing FB injection into retrosplenial cortex. C. Coronal section showing CTB 835 injection into mammillary bodies. D. Coronal dorsal subiculum section after 836 injections of Fast Blue into the retrosplenial cortex and FluoroGold into the 837 mammillary bodies. The open arrow head points to a single-labelled neuron 838 projecting to MB, the closed arrow head to single-labelled neuron projecting to 839 RSP, the open diamonds indicate double-labelled neurons. Abbreviations: CA1, 840 hippocampal field CA1; LMB, lateral mammillary nucleus; MMB, medial 841 mammillary nucleus; Rga, Rgb, granular retrosplenial cortex, subdivisions a and b, 842 respectively (collectively, area 29); Rdg, dysgranular retrosplenial cortex (area 30). 843 Scale bars =  $500 \mu m$ .

844

845 Figure 2. Quantification of extent and location of collateralizing neurons in dorsal 846 subiculum. Histogram illustrates the percentage of subiculum neurons projecting to 847 retrosplenial cortex that co-label with mammillary body tracer. For this analysis, 848 dorsal subiculum was divided by proximal-distal (R1-4) and anterior-posterior (AP) 849 locations (cell counts are presented in Extended Data Figure 2-1). Photomicrographs 850 depict dorsal subiculum (right hemisphere) at five AP levels (numbers indicate 851 distance from bregma in mm), the borders are color-coded to match the corresponding 852 bars in the histogram. The photomicrographs show pink double-labelled cells that 853 innervate both sites, red neurons projecting to MB, and blue neurons projecting to 854 RSP. Additional, higher magnification panels show labelling in more detail; FB (blue) 855 fills the cytoplasm while retrogradely transported CTB (red) remains in vesicles and 856 so appears granular. The open arrow head marks a single-labelled neuron projecting 857 to MB, the closed arrow head marks a single-labelled neuron projecting to RSP, the 858 open diamonds indicate double-labelled neurons. Scale bar =  $500 \mu m$  unless 859 otherwise specified.

860

Extended Data Figure 2-1. Numbers of Cholera Toxin Subunit B (CTB) and Fast
Blue (FB) positive cells within different proximal – distal positions (R1-R4) of the
dorsal and intermediate subiculum of the rat, including the number of double-labelled
cells. The case numbers and hemisphere of cell counts (R or L) are shown, along with
the percentage of subicular cells projecting to the retrosplenial cortex (RSP) that are
double labelled. Other abbreviations: MB, mammillary bodies.

867

Figure 3 Characterization of collateral-collateral transport. A1. Photomicrograph of 869 870 collateral-collateral transport following a Cholera Toxin B (CTB) injection into the 871 mammillary bodies. The section shows CTB terminal label in layers II and III of 872 granular retrosplenial cortex (area 29). The Nissl stained overlay (A2.) confirms the 873 abrupt border with dysgranular cortex (area 30). B. Coronal section showing terminal 874 label in dorsal pars lateralis (MMBl) and pars medianus (MMBmed) of the medial 875 mammillary nucleus following a retrosplenial CTB injection. Note, pia artefact has 876 been removed. C. Coronal section showing dense terminal label in the anterior 877 thalamic nuclei. **D.** Pattern of both retrograde and light terminal label in the entorhinal 878 cortex after a CTB injection into the mammillary bodies. Boxes, D2 and D3 879 correspond to higher magnification images of medial and lateral entorhinal cortex 880 respectively. E. Photomicrograph of dorsal subiculum following injection of an 881 anterograde tracer (BDA). F. Coronal section of retrosplenial cortex showing pattern 882 of BDA anterograde transport from dorsal subiculum. G. Coronal section from same 883 level of retrosplenial cortex as depicted in F., illustrating pattern of CTB terminal 884 label following CTB injection in mammillary bodies. Abbreviations: AD, 885 anterodorsal thalamic nucleus; AM, anteromedial thalamic nucleus; AV anteroventral thalamic nucleus; BDA, biotinylated dextran amine; LMB, lateral mammillary 886 887 nucleus; MB, mammillary bodies; MMBl, medial mammillary body, pars lateralis; 888 MMBm, medial mammillary body, pars medialis. Scale bars  $= 500 \mu m$  unless 889 otherwise specified. 890 891 Figure 4. Absence of collateral-collateral transport to retrosplenial cortex following a 892 Cholera Toxin B (CTB) injection into the mammillary bodies combined with lesion 893 involving the postcommissural descending fornix. A., B. Nissl stained sections, 1.56 894 mm behind bregma (according to Paxinos and Watson, 2005), showing

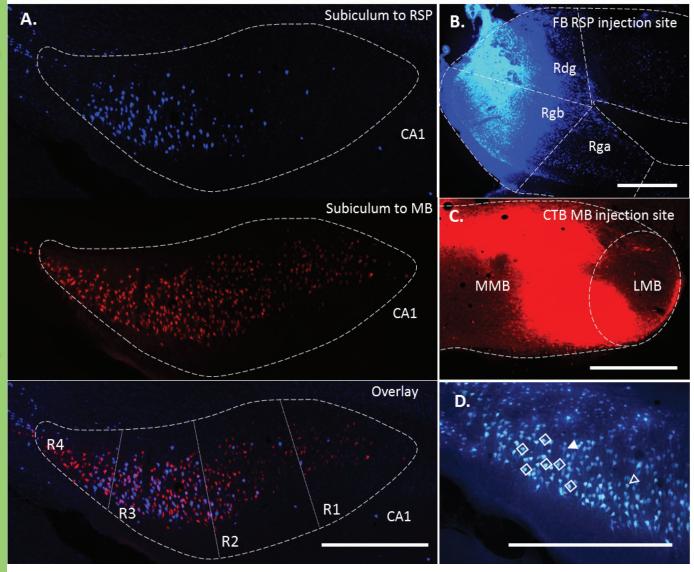
895 postcommissural fornix lesion (A.) and intact case (B.) respectively. C. Coronal 896 photomicrograph showing the very limited retrograde label in proximal dorsal 897 subiculum after a postcommissural fornix lesion. D. Typical appearance of retrograde 898 label in the dorsal subiculum in an intact case (CTB in mammillary bodies). E. Lack 899 of terminal label in the retrosplenial cortex after postcommissural fornix lesion. The 900 inset provides a comparison with an intact case. F., G. Retrogradely labelled neurons 901 in Gudden's ventral tegmental nucleus when the postcommissural descending fornix is lesioned (F.) or intact (G.) Note, while the label in D appears more restricted, it is 902 denser. Abbreviations: 3V,  $3^{rd}$  ventricle; opt, optic nerve. Scale bars =  $500\mu m$ . 903 904

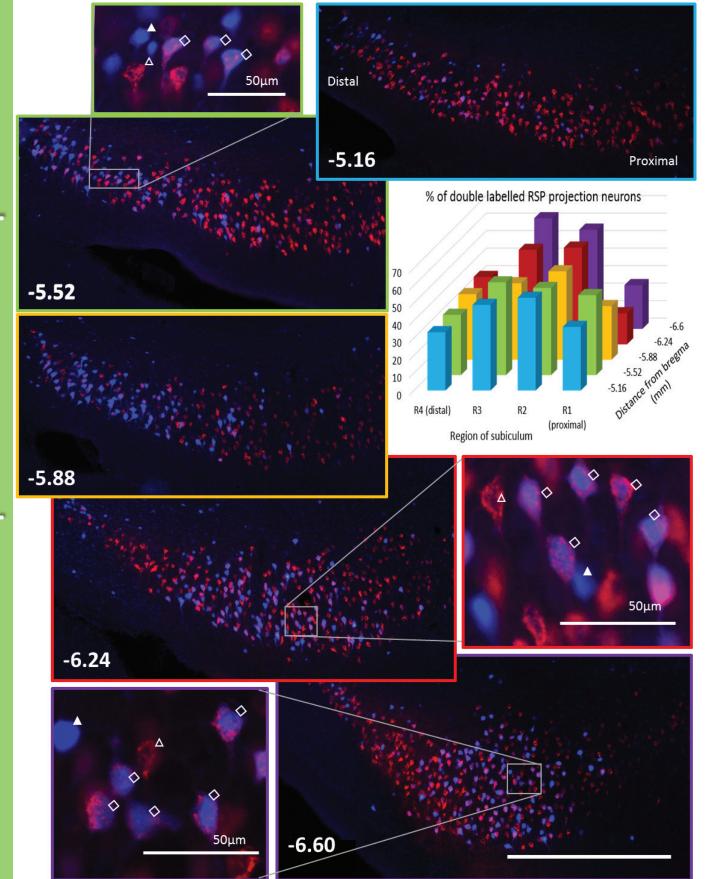
905 Figure 5. Cross-species comparisons. A. Coronal section showing Cholera Toxin B 906 (CTB) injection into mouse mammillary bodies. **B.** Coronal section showing Fast 907 Blue (FB) injection into mouse retrosplenial cortex. C. Coronal photomicrograph of 908 dorsal subiculum. The numerous double-labelled (pink) cells innervate both sites. 909 The open arrow head marks a single-labelled neuron projecting to MB, the closed 910 arrow head marks a single-labelled neuron projecting to RSP, the open diamonds 911 indicate double-labelled neurons. Inset depicts higher magnification of indicated 912 region. The open arrow head points to a single-labelled neuron projecting to MB, the 913 closed arrow head to a single-labelled neuron projecting to RSP, the open diamonds 914 indicate double-labelled neurons. Associated cell counts are presented in Extended 915 Data Figure 5-1. D1. Red terminal label in the granular retrosplenial cortex (area 29) 916 from collateral-collateral transport, alongside scattered retrogradely labelled cells in 917 retrosplenial cortex and the indusium griseum (IG). D2. A Nissl stained overlay of 918 section B1 shows the border between area 29 and area 30. The label is concentrated in 919 deep layer II and layer III of area 29. Abbreviations: LMB, lateral mammillary 920 bodies; MMB, medial mammillary bodies; PM, premammillary nucleus. Scale bar = 921 500µm unless otherwise specified. 922 923 Extended Data Figure 5-1. Numbers of Cholera Toxin Subunit B (CTB) and Fast 924 Blue (FB) positive cells within of the dorsal and intermediate subiculum of the 925 mouse, including the number of double-labelled cells. The case numbers and 926 hemisphere of cell counts (R or L) are shown, along with the percentage of subicular 927 cells projecting to the retrosplenial cortex (RSP) that are double labelled. Other 928 abbreviations: MB, mammillary bodies. 929 930 Figure 6. Neurochemical characterization of collateral-collateral terminals. A1. 931 Combined immunohistochemical signal for VGluT2 matching the distribution of 932 Cholera Toxin B (CTB) terminal label localized in superficial area 29. A2 shows at 933 greater magnification the separate CTB and VGluT2 label, with the overlay showing 934 co-localization within layers II and III of area 29. B1. Combined 935 immunohistochemical signal for neurotensin (NT) matching the distribution of 936 Cholera Toxin B (CTB) terminal label localized in superficial area 29. B2 shows at 937 greater magnification the separate CTB and NT label, with the overlay showing co-938 localization within layers II and III of area 29. Scale bar =  $500\mu$ m unless otherwise 939 specified. Note, pia artefact has been removed. Neurochemicals that did not co-940 localize with the CTB positive terminals are shown in Extended Data Figure 6-1. 941 942 **Extended Data Figure 6-1.** Series of coronal immunofluorescence images at the 943 level of the retrosplenial cortex in an animal with a Cholera Toxin B (CTB) injection 944 in the mammillary bodies. Left column: Green immunofluorescent label associated 945 with antibodies for VGluT1, GAD67, parvalbumin (PV), calretinin (CR), calbindin 946 (CB), and cholecystokinin (CCK). Middle column: CTB terminal label in the 947 retrosplenial cortex (area 29, layers II and III) highlighting the collateralizing 948 subiculum projections that were present in the same section as depicted in the left 949 column. Right column: The section overlay shows how the distribution of these 950 neurochemicals do not match the termination sites of the collateral projections from 951 the subiculum to area 29. Scale bar =  $500 \mu m$ . 952 953 Figure 7. Schematic depictions of described hippocampal network connectivity. 954 A. Ipsilateral and crossed collaterals from the subiculum reach the mammillary bodies 955 (MB) and retrosplenial cortex (RSP, area 29). Note, the subiculum projections to area

956 29 remain ipsilateral while collaterals to MB can remain ipsilateral or cross

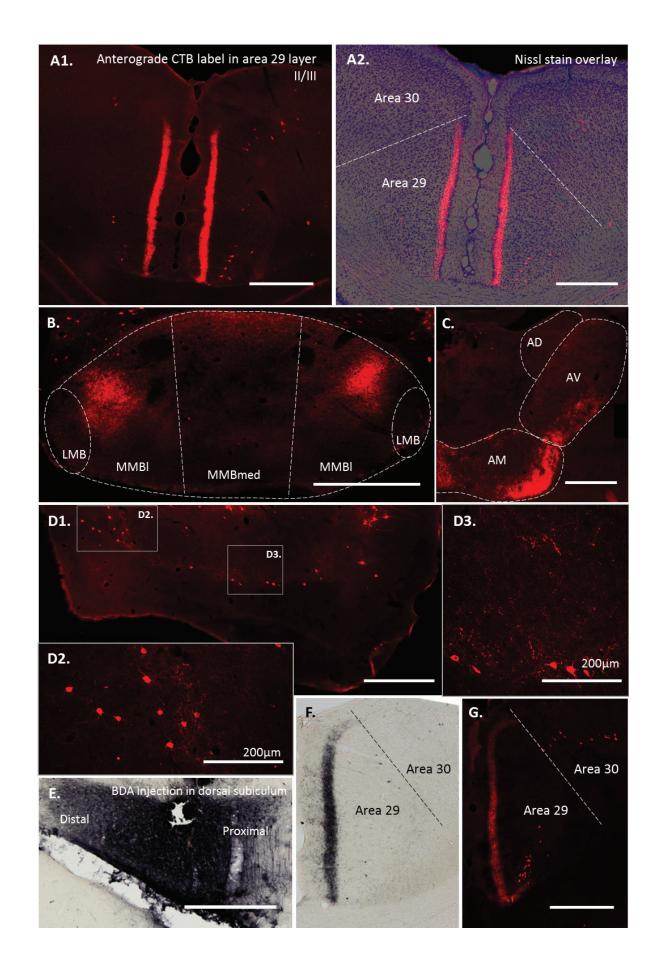
- 957 hemispheres. B. Updated hippocampal-limbic network ('Papez' circuit') showing the
- 958 ventral (subcortical), dorsal (cingulate), and new 'collateral' routes. Other
- 959 abbreviations: ATN, anterior thalamic nuclei; MTT, mammillothalamic tract.

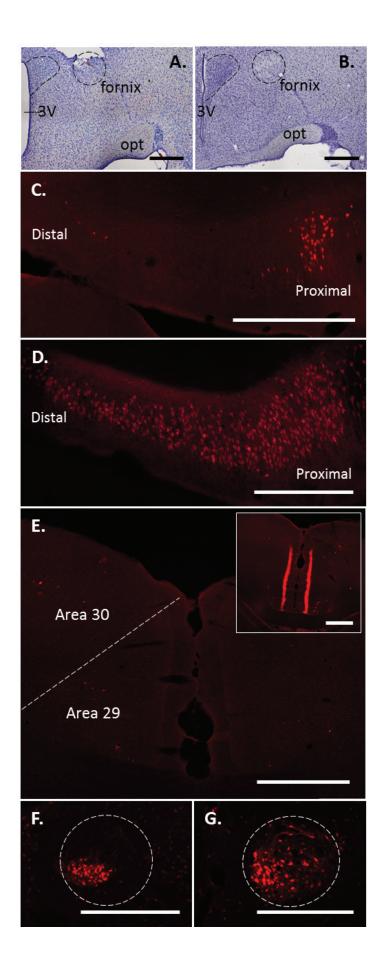






eNeuro Accepted Manuscript





# eNeuro Accepted Manuscript

